UC San Diego
UC San Diego Previously Published Works

Title

Synchronization of RF Data in Ultrasound Open Platforms (UOPs) for High-Accuracy and High-Resolution Photoacoustic Tomography Using the Scissors Programming Method.

Permalink

https://escholarship.org/uc/item/8q91q1xb

Journal

IEEE Transactions on Ultrasonics, Ferroelectrics and Frequency Control, 69(6)

Authors

Yim, Wonjun
Wu, Zhuohong
He, Tengyu
et al.

Publication Date

2022-06-01

DOI

10.1109/TUFFC.2022.3164371

Peer reviewed

HHS Public Access

Synchronization of RF data in ultrasound open platforms (UOPs) for high-accuracy and high-resolution photoacoustic tomography using the "Scissors" programming method

Lei Fu,

Department of NanoEngineering, University of California San Diego, La Jolla, CA 92093, USA

Zhicheng Jin,

Department of NanoEngineering, University of California San Diego, La Jolla, CA 92093, USA

Baiyan Qi,

Materials Science and Engineering Program, University of California San Diego, La Jolla, CA 92093, USA

Wonjun Yim,

Materials Science and Engineering Program, University of California San Diego, La Jolla, CA 92093, USA

Zhuohong Wu,

Department of NanoEngineering, University of California San Diego, La Jolla, CA 92093, USA

Tengyu He,

Materials Science and Engineering Program, University of California San Diego, La Jolla, CA 92093, USA

Jesse V. Joksert

Department of NanoEngineering, University of California San Diego, La Jolla, CA 92093, USA; Materials Science and Engineering Program, University of California San Diego, La Jolla, CA 92093, USA; Department of Radiology, University of California San Diego, La Jolla, CA 92093, USA.

Abstract

Synchronization is important for photoacoustic tomography but some fixed delays between the data acquisition and the light pulse are a common problem degrading imaging quality. Here, we present a simple yet versatile method named "Scissors" to help synchronize ultrasound open platforms (UOPs) for photoacoustic imaging. Scissors is a programmed function that can cut or add a fixed delay to RF data and thus synchronize it before reconstruction. Scissors applies the programmable metric of UOPs and has several advantages: It is compatible with many setups regardless of the synchronization methods, light sources, transducers, and delays. The synchronization is adjustable in steps reciprocal to the UOPs' sampling rate (20-ns step with 50-MHz sampling rate). Scissors works in real-time photoacoustic imaging, and no extra hardware is needed. We programmed Scissors in Vantage UOP (Verasonics), and then imaged two 30-μm

Corresponding author: Jesse V. Jokerst, jjokerst@ucsd.edu.

nichrome wires with a 20.2-MHz central frequency transducer. The PA image was severely distorted by a 828-ns delay; over 90% delay was caused by our Q-switch laser. The axial and lateral resolution are 112 μm and 167 μm, respectively, after using Scissors. We imaged a human finger *in vivo* and the imaging quality is tremendously improved after solving the 828-ns delay by using Scissors.

Keywords

Photoacoustic imaging; Synchronization; Ultrasound open platform; Programming

1. Introduction

Photoacoustic (PA) tomography is a hybrid imaging *modality* that uses a sound-in and light-out approach [1]. When a pulse laser illuminates exogenous or endogenous contrast agents, the absorbed light generates heat energy and induces acoustic waves that can be detected by an ultrasound transducer [2]. Photoacoustic tomography offers high spatiotemporal resolution and deep penetration and holds great promise for biomedical applications [3, 4]. There are two different types of photoacoustic tomography: One applies a single transducer element that moves across the sample and collects the radio frequency (RF) signal at each location. This is cost-effective but slow [5]. A second approach uses a transducer array including linear arrays [6], circular arrays [3, 7], or 2D arrays [8] with tens or hundreds of elements to collect the RF signal simultaneously. This method is expensive but provides much higher frame rate for real-time studies [9]; however, this method requires multi-channel ultrasound data acquisition systems capable of receiving and processing massive RF signal in parallel [10].

Commercial ultrasound open platforms (UOP) with hundreds of channels are a powerful tool in photoacoustic research [11]. UOPs provide great flexibility in system configuration for both commercial and homemade transducers, real-time direct accessibility to RF and imaging data, and easy incorporation of customized algorithms/functions [12]. It is important for UOPs to provide trigger channels for synchronization in photoacoustic imaging [13, 14]. Nevertheless, synchronizing UOP and pulsed light source can still be a big challenge. A common example is the Verasonics Vantage UOP and OPO laser (OPOTEK). There are three possible fixed delays in the photoacoustic imaging depending on the setup: 1) There is a delay between Q-switch-in trigger and laser pulse—the inherent Q-switch trigger propagation time and the laser resonator build-up time in the laser (750 ns with our laser) [15]; 2) Acquisition takes time to begin when Vantage receives a trigger from laser, i.e., there is a delay in the overhead of direct memory access (DMA) initiation and termination (15 μs in our case) [8]; and 3) There is delay when the Vantage output trigger needs to be converted (150 ns with our pulse converter). The Vantage system can only produce negative 1-μs-wide triggers while some lasers only recognize longer or positive triggers [16]. Any of the above delays can cause asynchronization degrading the imaging quality. For example, a 200-ns asynchronization between data acquisition and light pulse will shift the PA signal by approximately 300 μm assuming the speed of sound is 1500 m/s. The asynchronization can dramatically decrease the resolution of high-frequency

transducers, e.g., even a 200-ns asynchronization with a 30 MHz transducer can dramatically compromise image quality. Moreover, the PA data will appear offset from its actual position with worse resolution. This is particularly conspicuous when overlaid with the ultrasound image.

Several methods have been proposed to solve this issue. Yoon et al. suggested using the light pulse to trigger data acquisition for synchronization [16], but the data acquisition (DAQ) system may need time for setup after receiving a trigger as described above. Wu et al. proposed two algorithms that synchronize clinical ultrasound scanner for photoacoustic without using triggers [17]. However, this method is limited to post-processing, which is time-consuming. A potential solution to solve the delay issue is to add more delay to the original to synchronize with the next subsequent event. For example, when data acquisition starts 1-ms later than light pulse in 20 Hz, the data acquisition can be further delayed for 49 ms (49 ms= 1 s/20 Hz - 1 ms) to synchronize with the next light pulse. However, this method can cause annoying jitter [12].

In this study, we propose a versatile method named Scissors that can help synchronize an UOP with a light source for photoacoustic imaging: Scissors cuts or adds delays in the RF data for real-time synchronization. Adding a delay to the photoacoustic RF data can extend the focus depth of photoacoustic microscopy [18] and correct the speed of sound in tissue [19]. Here, we use this method for synchronization, and found that it offers multiple advantages: 1) Scissors works in real-time photoacoustic imaging, and no extra hardware is needed. 2) The synchronization is adjustable in steps reciprocal to the UOPs' sampling rate (20-ns step by 50 MHz sampling rate). 3) Scissors is broadly compatible with many setups regardless of the synchronization methods, light sources, transducers, or delays.

2. Methods

2.1 Scissors

We programmed Scissors as an external function of Vantage UOP (Verasonics, Inc., Kirkland, WA, USA). A sample script 'SetUpL11_4vFlashAngPA.m' was upgraded to incorporate Scissors. Main objects including Receive, Recon, ReconInfo, Process, and Events were redefined. A new function that can delay laser pulse in 4-ns steps was added. We fixed two bugs from the sample script that make the Vantage output triggers unstable. Our script ran with Vantage software release '4.5.4-2108261500' with Matlab 2020b, and it is available in the Verasonics Community portal website (https://verasonicscommunity.com).

2.2 Vantage ultrasound open platform.

We used the Vantage system to receive, process, and reconstruct the PA and ultrasound signal. It offers trigger in-and-out channels for synchronization. It has 256 channels in parallel, with a 14-Bit (analog digital converter) ADCs operating at 62.5 MHz, which limits the maximum sampling rate to be 62.5 MHz. The Vantage system has a master clock working at 250 MHz.

2.3 Hardware.

A commercially available transducer (L22-14vX; Verasonics, Inc., Kirkland, WA, USA) received the PA signal with central frequency of 20.2 MHz and bandwidth of 14-22 MHz. A tunable OPO laser (OPOTek) is the light source operating at 680 – 970 nm at 20Hz. The wavelength is fixed at 850 nm. The pulse width is 5-7 ns, and the pulse energy is 13 mJ. We used a fiber bundle (10 2.5-mm-diameter fibers) to couple light to the sample. A function generator (33500B, Keysight) operating in burst mode was used to convert the Vantage output trigger into positive 100-µs Q-switch trigger. A photodetector (DET10A2, Thorlabs) was used to detect the laser pulse. An oscilloscope (TDS 2022C, Tekronix) with two channels was used to capture all the triggers including Verasonics output trigger (Data acquisition) and the Q-switch trigger from the function generator.

2.4 Ex vivo validation.

We used two nichrome heater wires (30 µm diameter) as imaging sample. The wires were put into a 3D-printed holder that keeps them parallel and 1.2 mm apart [20]. The acquisitions were averaged twice decreasing the frame rate from 20 Hz to 10 Hz. The speed of sound is set at 1510 m/s, which is an important variable for high-frequency imaging and is associated with the purity of water and temperature [21, 22]. We defined the FWHM (full width at half maximum) of the lateral and axial amplitude distributions of the wires as the axial and lateral resolution, respectively [23].

3. Discussion & Results

We first introduce a common setup for PA imaging using the Verasonics Vantage system that has fixed delays that lead to asynchronization and impact quality imaging. We then describe our Scissors method, strategies to perform it in real time in programming, and then validate it *ex vivo* and *in vivo*. Although Scissors was used with the Vantage system in this work, other UOPs can be used as well because they have similar protocols for programming and synchronization.

3.1 System setup and Imaging delays

There are various ways to synchronize a Q-switched laser with the Vantage system [13, 14]: The most popular one with the least jitter uses the Vantage system to trigger the laser and is shown in Fig. 1(a) [12]. Its trigger flow is shown in Fig. 1(b). All the triggers are measured by using an oscilloscope. Take the OPO Q-switched laser as an example: The Vantage system receives a flash-lamp output trigger from the laser and waits for 250 µs for optical laser built-up. At 250 µs, the Vantage system starts data acquisition and generates a negative output trigger simultaneously. The output trigger can work as a Q-switch trigger which, unfortunately, is negative and only 1-µs wide. It is not recognizable by many lasers. Thus, we used a function generator to convert the output trigger as a Q-switch trigger to the laser [16]. ① ② ③ are the delays in the whole process: ①: Delay between flash-lamp trigger and DAQ output trigger (250 µs) for laser optical build-up; ② Delay introduced by the function generator (170 ns), which converts the Q-switch trigger. ③ Delay between Q-switch trigger and laser pulse (745 ns). These delays can be different with different laser sources and pulse inverters. ② and ③ collectively lead to asynchronization between the data

acquisition and laser pulse in our case. We measured this total delay across 10 replicates as shown in Fig. 1(c) (915 ns on average with a jitter [24] of 4 ns). Note that laser jitter is different from the asynchronization that we are solving. A jitter of 4 ns is considered to be small: PA signal would travel ~6 μm in 4 ns (1490 m/s = speed of sound). Therefore, the effect of jitter should not be observable because our lateral and axial resolution are much larger than 6 μm.

To reveal the impact of this total delay in PA imaging, we acquired PA and ultrasound (PA-US) images of two nichrome wires with a 20.2-MHz transducer (Methods). Fig. 1(d) is the PA-US image in a cross-section view. The PA image is coded in red and overlaid with the ultrasound image in gray. Clearly, the PA imaging quality is tremendously degraded by the asynchronization because the wires are largely distorted into two curves. Moreover, the wires are dislocated in the PA image where they appear 1.25 mm below their true position in the ultrasound image. The dislocation indicates that the PA acquisition started earlier, which in turn can help measure the total delay without using any extra hardware. By dividing the dislocation with the speed of sound, we have (1.25 mm)/(1510 m/s) = 828 ns, which is 87 ns different from measuring the triggers (915 ns) in Fig. 2(b). Here, we identified a 828-ns delay underlying the asynchronization.

3.2 Programming Scissors for synchronization

We programmed an external function named Scissors to help synchronize the RF data with light pulse in real time. Since data acquisition starts earlier than the laser pulse causing the asynchronization in Fig. 1, we use Scissors to cut away the extra RF data collected before the light pulse and keep the rest RF data for reconstruction as shown in Fig. 2(a). The lateral axis represents the element index of a transducer and the axial axis represents time. Each grid takes 16 ns when the sampling rate is 62.5 MHz: (1 second) / (62.5 MHz) =16 ns. The location of Scissors in pixels is determined by the Eq (1):

$$(Scissors\,Location,\,Remain) = \frac{Delay}{16\,ns} \tag{1}$$

$$Laser\,Delay = \frac{16\,ns - Remain}{4\,ns} \tag{2}$$

Eq. (1) indicates that the remaining asynchronization is the variable *Remain*, which is reduced from 828 ns to less than 16 ns. The Scissors function can also add delays to compensate the RF data in cases where data acquisition starts later than the laser pulse. Vantage system has a master clock running at 250 MHz, which allows the delay of its output trigger; hence, the Q-switch trigger and laser pulse move in steps of 4 ns (1 Second /250 MHz = 4 ns) relative to its data acquisition. In other words, we can move the light pulse closer to the second row of the RF data (Fig. 2(b)) in less than 4 ns as determined in steps by Eq. (2). The first row is cut away. Such a 4-ns synchronization is not necessary for most high-frequency transducers. Nevertheless, the idea of combining Scissors and laser delaying could bring more flexibilities for other UOPs and setups. All the channels have the same

and fixed delay. This delay is measurable as described in Fig. 1. Scissors can automatically compensate for this delay.

The programming flow of using Scissors in the Vantage system is shown in Fig. 2(c). Ultrasound imaging and PA imaging are performed separately, and the US and PA RF data are transferred to the computer using two 'transferToHost' commands separately. The ultrasound RF data are transferred to an ultrasound receive buffer and the PA RF data are transferred to a PA receive buffer. Scissors is defined as an external function, which cuts the RF data from the PA buffer and transfers the data into a PA dummy receive buffer. The Vantage system uses the PA dummy buffer for reconstruction. The three cartoon images show that asynchronized RF data causes distorted and dislocated PA image and how Scissors can solve these issues. To illustrate, all processes can happen in real-time in UOPs not just in post-processing. The script is shared on Verasonics community website.

3.3 Phantom wire imaging

We evaluate our Scissors method by using two nichrome wires as sample and a 20.2 MHz transducer. The wires are put in water 10 mm underneath the transducer with 1.2 mm apart. We acquired PA-US images with Scissors cutting the RF data at different time with respect to laser pulse: −576 ns, −384 ns, −192 ns, 0 ns (synchronized case), 96 ns, 192 ns, 384 ns, and 576 ns as shown in Fig. 3. The nichrome wires are largely distorted and dislocated in the PA images when Scissors are 576 ns away from the laser pulse (Fig. 3(a) and 3(h)). As the position behind cut is moved closer to the laser pulse from 576 ns to 192 ns (Fig. 3(a) to 3(d)), the imaging quality is tremendously improved: The image distortion is solved, and the wires in the PA image move closer to their real position in the ultrasound image. When Scissors and the light pulse are at the same time as shown in Fig. 3(d), the PA image is well overlaid with the ultrasound image, where the two wires are shown as two tiny spots with the highest lateral resolution.

We measured the lateral and axial resolution by FWHM in the synchronized case to be 112 um and 167 μm, respectively (Section 2.4). The lateral and axial resolution in the ultrasound imaging are 91 um and 120 μm, respectively. The lateral and axial resolution of PA imaging with Scissors moving at different time with respect to light pulse is shown in Fig. 3(i). The depth of the left wire with respect to its real depth is also plotted in Fig. 3(j). Obviously, the asynchronization between RF data and light pulse causes lateral distortion of the image and mainly impacts the lateral resolution of PA imaging and the depth of the wires in the PA image. The axial resolution does not change significantly. Fig. 3 proves the super flexibility of our Scissors method in adjusting the delay step by step from asynchronization to synchronization.

3.4 Tissue imaging

We also evaluated our Scissors method *in vivo* by imaging a human finger with a 30 MHz transducer (LZ 400, Visualsonics, Canada). The finger is unfixed in water 10 mm underneath the transducer. We acquired PA-US images without and with Scissors cutting the delay of 828 ns. Similar to Fig. 3(a), the speckle in the PA image is laterally distorted in the PA images without using Scissors (Fig. 4(a)). Moreover, the skin surface is dislocated from the

ultrasound image. The imaging quality is tremendously improved after using Scissors (Fig. 4(c)): The lateral distortion is solved, and the skin surface in the PA image is at the same depth within the ultrasound image. Our in vivo experiment proves that the Scissors method can fix the delay and improve the imaging quality for more biomedical applications.

4. Conclusion

In conclusion, this study demonstrated the ability of Scissors to help compensate the delay between ultrasound open platforms (UOPs) with light source for photoacoustic imaging. Scissors relies on the great flexibility of UOPs in programming and manipulating the RF data, which allows us to cut or add delays to RF data in real time and thus it is compatible with many setups in photoacoustic imaging. We imaged two nichrome wires by using Verasonics Vantage open platform and a 20.2 MHz transducer. The lateral and axial resolution are as high as 112 μm and 167 μm after synchronization, separately.

Acknowledgments

Biographies
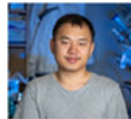
Lei Fu is a PhD student in the Nanoengineering department at UC San Diego.

He received his B.S and M.E. degree from Jiangnan University in China. His previous work mainly concentrates on Optical Coherence Tomography(OCT) especially OCT angiography. Currently he is working on photoacoustic imaging.

Zhicheng Jin is a postdoctoral scholar in the Department of NanoEngineering at UC San Diego.

He graduated from Lanzhou University in 2015 with a B.S. in Chemistry.He then received his Ph.D. in 2020 under the supervision of Prof. Hedi Mattoussi at the Florida State University, where he worked on designing functional nanomaterials and developing FRET-based nanosensors for probing MMP enzymes. His research in Jokerst group focuses on the synthesis of functional polypeptides as photoacoustic contrast agents for detecting Mpro protease.

Baiyan Qi a PhD student in Materials Science and Engineering program at UCSD.

She received her B.S. degree in Physics from Nanjing University in China. Her previous research focused on stretchable wearable electronics. She is currently working on ultrasonic and photoacoustic healthcare imaging.

Wonjun Yim is a Ph.D. candidate in Materials Science and Engineering program at UCSD.

He finished his undergraduate degree at Yonsei University, South Korea. After that, he did his masters at UC Berkeley where he studied material science engineering in depth. Currently, he is working on polyphenol-based nanoparticle synthesis for biomedical applications.

Zhuohong Wu Joined Prof. Jokerst lab in 2021.

He is working on the development of a multimodal platform based on the metal–phenolic materials for biomedical applications. He is currently a PhD student in the Department of NanoEngineering at UCSD.

Tengyu He is a PhD candidate in the Materials Science and Engineering graduate program at UCSD.

He received his M.S. degree in Materials Science and Engineering from the University of Chinese Academy of Sciences. At UCAS he conducted research in the application of nanomaterials in the design of stretchable electronics. He is currently studying nanomaterials for cancer theranostics and thrombus imaging.

Jesse V. Jokerst is a Professor in the Department of NanoEngineering at UC San Diego. Dr. Jokerst graduated *cum laude* from Truman State University in 2003 with a B.S. in Chemistry and completed a Ph.D. in Chemistry at The Uni- versity of Texas at Austin in 2009. Jesse was a postdoc at Stanford Radiology from 2009 to 2013 and was an Instructor in that same department from 2013–2015. Jesse started at UCSD in July of 2015, and he has received the NIH K99/R00 Pathway to Independence Award, the NIH New Innovator Award, the NSF CAREER Award, and Stanford Radiology Alumni of the Year Award. He is the PI of multiple NIH grants and NSF grants, and serves on the Editorial Advisory Board of *ACS Applied Nano Materials* and *Nanoscale*.

Data availability

Data can be requested from the authors at any time. Script used in this study is available in the Verasonics Community portal website (https://verasonicscommunity.com).

References

[1]. Wang LHV and Yao JJ, "," (in English), Nature Methods, vol. 13, no. 8, pp. 627–638, Aug 2016, doi:10.1038/Nmeth.3925. [PubMed: 27467726]

[2]. Das D, Sharma A, Rajendran P, and Pramanik M, "Another decade of photoacoustic imaging," (in English), Phys Med Biol, vol. 66, no. 5, Mar 7 2021, doi: ARTN 05TR01 10.1088/1361-6560/abd669.

[3]. Lin L et al. "Single-breath-hold photoacoustic computed tomography of the breast," (in English), Nat Commun, vol. 9, Jun 15 2018, doi: ARTN 2352 10.1038/s41467-018-04576-z.

[4]. Moore C et al. "Photoacoustic imaging for monitoring periodontal health: A first human study," Photoacoustics, vol. 12, pp. 67–74, Dec 2018, doi: 10.1016/j.pacs.2018.10.005. [PubMed: 30450281]

[5]. Sharma A, Kalva SK, and Pramanik M, "A Comparative Study of Continuous Versus Stop-and-Go Scanning in Circular Scanning Photoacoustic Tomography," (in English), Ieee J Sel Top Quant, vol. 25, no. 1, Jan-Feb 2019, doi: Artn 7100409 10.1109/Jstqe.2018.2840320.

[6]. Roy K et al. "Body Conformal Linear Ultrasound Array for Combined Ultrasound and Photoacoustic Imaging," (in English), Proceedings of the 2020 Ieee International Ultrasonics Symposium (Ius), 2020. [Online]. Available: <Go to ISI>://WOS:000635688900155.

[7]. Na S et al. "Massively parallel functional photoacoustic computed tomography of the human brain," (in English), Nat Biomed Eng, May 31 2021, doi: 10.1038/s41551-021-00735-8.

[8]. Yu JS, Yoon H, Khalifa YM, and Emelianov SY, "Design of a Volumetric Imaging Sequence Using a Vantage-256 Ultrasound Research Platform Multiplexed With a 1024-Element Fully Sampled Matrix Array," (in English), Ieee T Ultrason Ferr, vol. 67, no. 2, pp. 248–257, Feb 2020, doi: 10.1109/Tuffc.2019.2942557.

[9]. Sivasubramanian K and Pramanik M, "High frame rate photoacoustic imaging at 7000 frames per second using clinical ultrasound system," (in English), Biomed Opt Express, vol. 7, no. 2, pp. 312–323, Feb 1 2016, doi: 10.1364/Boe.7.000312. [PubMed: 26977342]

[10]. Upputuri PK and Pramanik M, "Recent advances toward preclinical and clinical translation of photoacoustic tomography: a review," J Biomed Opt, vol. 22, no. 4, p. 41006, Apr 1 2017, doi: 10.1117/1.JBO.22.4.041006. [PubMed: 27893078]

[11]. Boni E, Yu ACH, Freear S, Jensen JA, and Tortoli P, "Ultrasound Open Platforms for Next-Generation Imaging Technique Development," IEEE Trans Ultrason Ferroelectr Freq

Control, vol. 65, no. 7, pp. 1078–1092, Jul 2018, doi: 10.1109/TUFFC.2018.2844560. [PubMed: 29993364]

[12]. Kratkiewicz K, Manwar R, Zhou Y, Mozaffarzadeh M, and Avanaki K, "Technical considerations in the Verasonics research ultrasound platform for developing a photoacoustic imaging system," (in English), Biomed Opt Express, vol. 12, no. 2, pp. 1050–1084, Feb 1 2021, doi: 10.1364/Boe.415481. [PubMed: 33680559]

[13]. Yoon H and Emelianov SY, "Combined Multiwavelength Photoacoustic and Plane-Wave Ultrasound Imaging for Probing Dynamic Phase-Change Contrast Agents," IEEE Trans Biomed Eng, vol. 66, no. 2, pp. 595–598, Feb 2019, doi: 10.1109/TBME.2018.2849077. [PubMed: 29993455]

[14]. Wei CW et al. "Real-time integrated photoacoustic and ultrasound (PAUS) imaging system to guide interventional procedures: ex vivo study," IEEE Trans Ultrason Ferroelectr Freq Control, vol. 62, no. 2, pp. 319–28, Feb 2015, doi: 10.1109/TUFFC.2014.006728. [PubMed: 25643081]

[15]. I. RMPC lasers. "Why is a low jitter feature important in actively Q-switch dpss lasers?" https://blog.rpmclasers.com/why-is-a-low-jitter-feature-important-in-actively-q-switched-dpss-lasers (accessed.

[16]. Yoon H, Zhu YYI, Yarmoska SK, and Emelianov SY, "Design and Demonstration of a Configurable Imaging Platform for Combined Laser, Ultrasound, and Elasticity Imaging," (in English), Ieee T Med Imaging, vol. 38, no. 7, pp. 1622–1632, Jul 2019, doi: 10.1109/Tmi.2018.2889736.

[17]. Wu YX, Zhang HCK, Kang J, and Boctor EM, "An economic photoacoustic imaging platform using automatic laser synchronization and inverse beamforming," (in English), Ultrasonics, vol. 103, Apr 2020, doi: ARTN 106098 10.1016/j.ultras.2020.106098.

[18]. Li ML, Zhang HE, Maslov K, Stoica G, and Wang LV, "Improved in vivo photoacoustic microscopy based on a virtual-detector concept," Opt Lett, vol. 31, no. 4, pp. 474–6, Feb 15 2006, doi: 10.1364/ol.31.000474. [PubMed: 16496891]

[19]. Yoon C, Kang J, Han S, Yoo Y, Song TK, and Chang JH, "Enhancement of photoacoustic image quality by sound speed correction: ex vivo evaluation," Opt Express, vol. 20, no. 3, pp. 3082–90, Jan 30 2012, doi: 10.1364/OE.20.003082. [PubMed: 22330545]

[20]. Arconada-Alvarez SJ, Lemaster JE, Wang JX, and Jokerst JV, "The development and characterization of a novel yet simple 3D printed tool to facilitate phantom imaging of photoacoustic contrast agents," (in English), Photoacoustics, vol. 5, pp. 17–24, Mar 2017, doi: 10.1016/j.pacs.2017.02.001. [PubMed: 28239554]

[21]. von Rohden C, Fehres F, and Rudtsch S, "Capability of pure water calibrated time-of-flight sensors for the determination of speed of sound in seawater," J Acoust Soc Am, vol. 138, no. 2, pp. 651–62, Aug 2015, doi: 10.1121/1.4926380. [PubMed: 26328683]

[22]. Lin CW and Trusler JP, "The speed of sound and derived thermodynamic properties of pure water at temperatures between (253 and 473) K and at pressures up to 400 MPa," J Chem Phys, vol. 136, no. 9, p. 094511, Mar 7 2012, doi: 10.1063/1.3688054. [PubMed: 22401456]

[23]. Li X, Wei W, Zhou QF, Shung KK, and Chen ZP, "Intravascular photoacoustic imaging at 35 and 80 MHz," (in English), J Biomed Opt, vol. 17, no. 10, Oct 2012, doi: Artn 106005 10.1117/1.Jbo.17.10.106005.

[24]. Asadollahi A et al. "Axial accuracy and signal enhancement in acoustic-resolution photoacoustic microscopy by laser jitter effect correction and pulse energy compensation," (in English), Biomed Opt Express, vol. 12, no. 4, pp. 1834–1845, Apr 1 2021, doi: 10.1364/Boe.419564. [PubMed: 33996201]
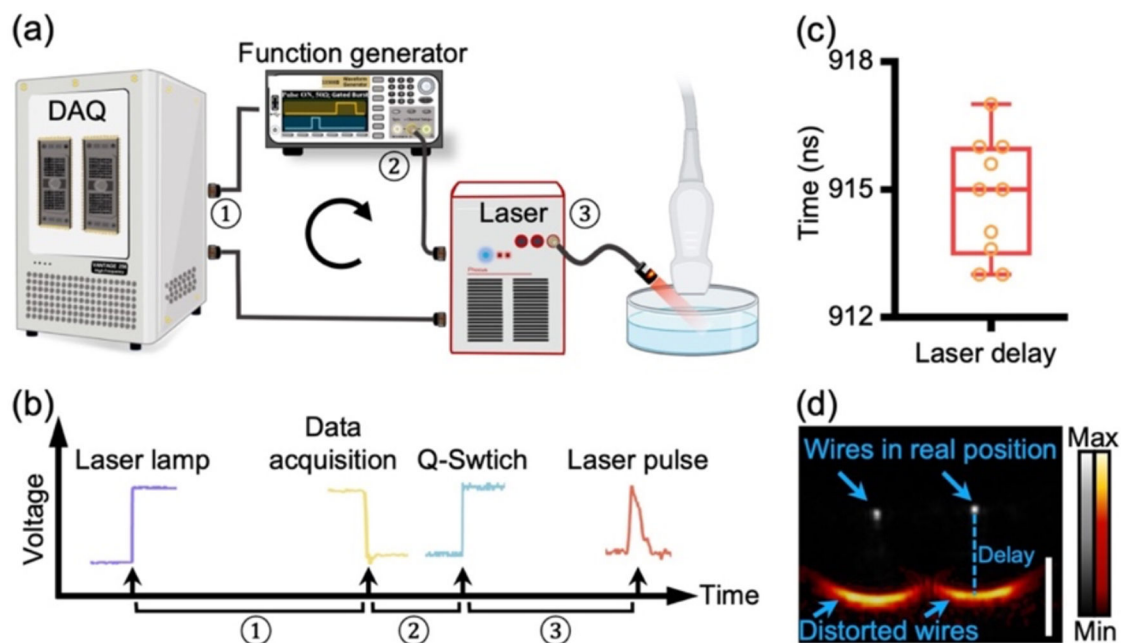
Fig. 1. Asynchronization degrades PA imaging quality.
a) System setup. Vantage system receives flash-lamp trigger from laser, waits for certain time for the optical-buildup of the laser, and then starts data acquisition. Upon data acquisition, Vantage system generates a negative output trigger. Function generator inverts the output trigger to positive Q-switch trigger and fires laser pulse. ① ② ③ are the delays introduced by Vantage system, function generator and Laser, respectively. b) Trigger flow and Delays. ① — Delay between Laser-lamp trigger and Vantage output trigger (250 μs), ② — Delay between Vantage output trigger and Q-switch trigger (170 ns), and ③ — Delay between Q-switch trigger and laser pulse (745 ns). c) Total delay between the Verasonics output trigger and laser pulse in 10 repeated measurements (*n*=10). d) PA image and ultrasound image of two nichrome wires. PA image is in red code and overlaid to the ultrasound image in gray. The wires are 10 mm underneath the transducer and 12 mm apart from each other. The scale bar is 1 mm.
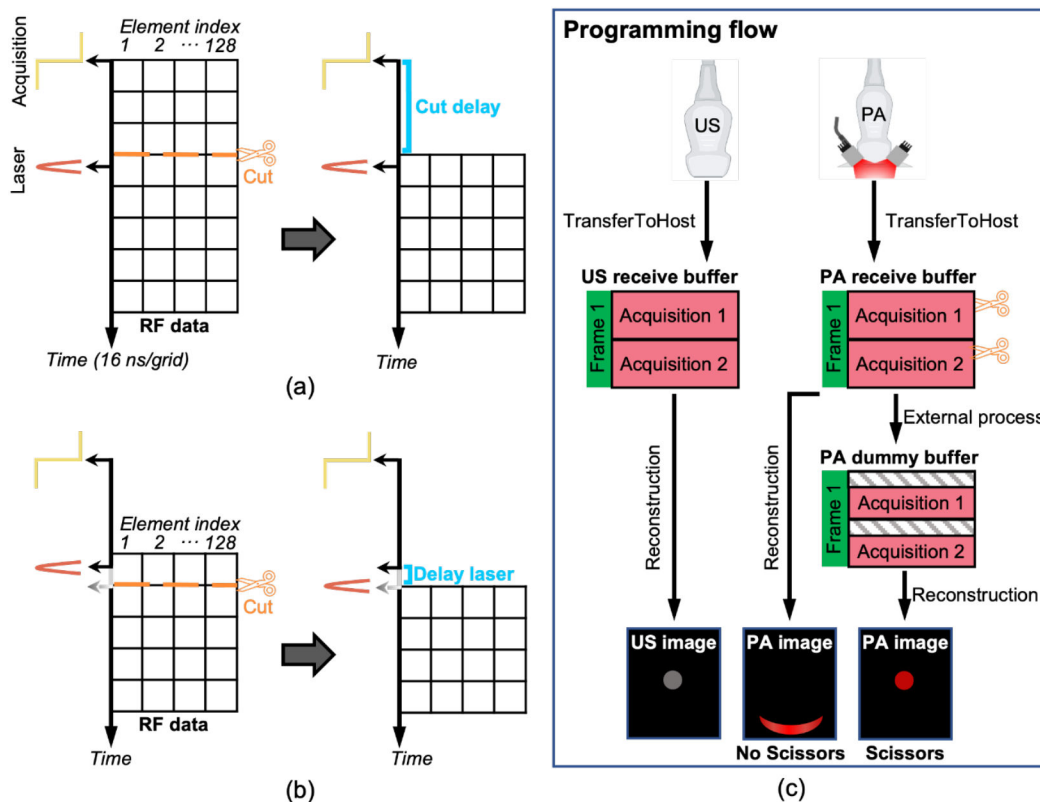
Fig. 2. Scissors cuts RF data for synchronization.

a) Synchronization in less than 16 ns. RF data collected before laser pulse are cut away. Each grid represents one digital-converted RF data collected by one element, and it takes 16 ns for 62.5 MHz sampling rate. Lateral axis represents the element index and axial axis represents time. b) Higher-level synchronization in less than 4 ns. Laser pulse is delayed by delaying its Q-switch trigger in steps of 4 ns until it synchronizes with the second row of RF data. The first row is cut away. c) Flow chart of sequence programming of one frame with Scissors and Vantage UOP system. Ultrasound imaging and PA imaging are conducted independently and sequentially. Scissors cut the RF data in PA receive buffer and put it into a PA dummy buffer for reconstruction.
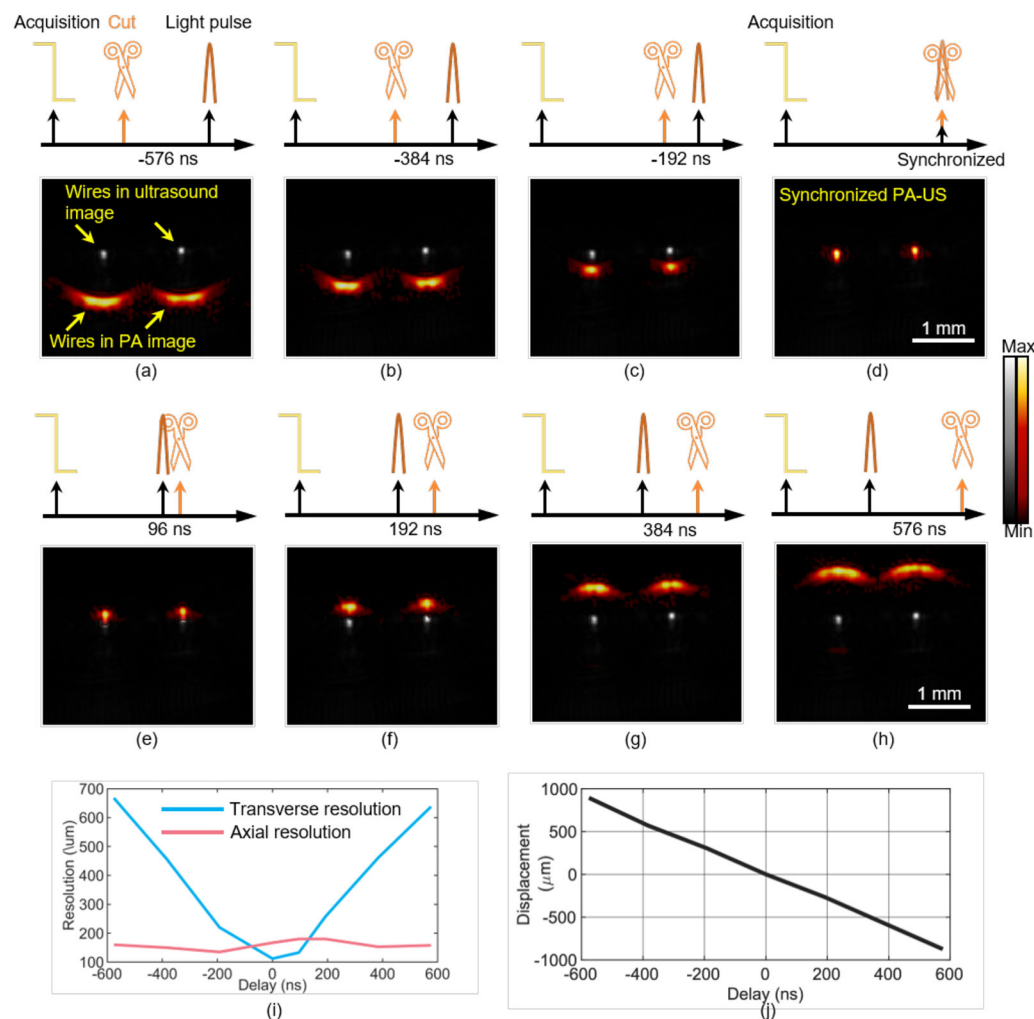
Fig. 3. Validating Scissors in *ex vivo* imaging.

Two nichrome wires were used as the sample. RF data are cut at different time with respect to laser pulses and PA-US images are acquired in real time (a–g): −576 ns (a), −384 ns (b), −192 ns (c), 0 ns (d), 96 ns (e), 192 ns (f), 384 ns (g), and 576 ns (h). Panel (i) shows the lateral resolution (blue line) and axial resolution (red line) when Scissors cuts RF data at different delays relative to the laser pulse. (j) The displacement of the left wire from its true depth in the PA image at different delays.
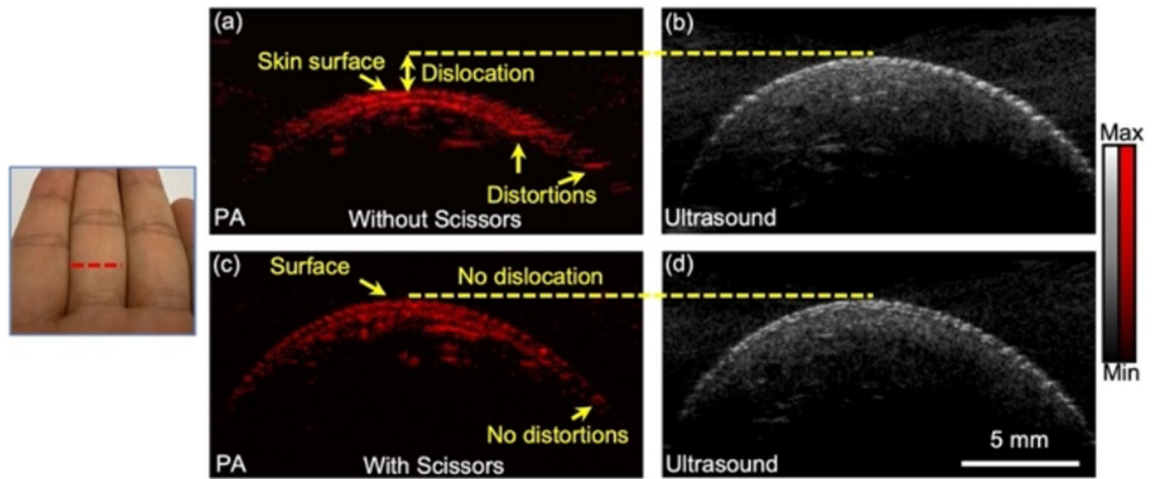
Fig. 4. Photoacoustic imaging of human finger without Scissors (a) and with Scissors (c).
(b) and (d) are the corresponding ultrasound images.